
Sample-Efficient Imitation Learning via Generative Adversarial Nets

Lionel Blondé, Alexandros Kalousis
University of Geneva, HES-SO, Switzerland
{lionel.blonde, alexandros.kalousis}@unige.ch

Abstract

Recent work in imitation learning articulate their formulation around the GAIL architecture, relying on the adversarial training procedure introduced in GANs. Albeit successful at generating behaviours similar to those demonstrated to the agent, GAIL suffers from a high sample complexity in the number of interactions it has to carry out in the environment in order to achieve satisfactory performance. In this work, we dramatically shrink the amount of interactions with the environment by leveraging an off-policy actor-critic architecture. Additionally, employing deterministic policy gradients allows us to treat the learned reward as a differentiable node in the computational graph, while preserving the model-free nature of our approach. Our experiments span a variety of continuous control tasks.

1 Introduction

Reinforcement learning (RL) is a powerful and extensive framework enabling a learner to tackle complex continuous control tasks (Sutton and Barto, 2017). Leveraging strong function approximators such as multi-layer neural networks, deep reinforcement learning alleviates the customary preliminary workload consisting in hand-crafting relevant features for the learning agent to work on. While being freed from this engineering burden opens up the framework to an even broader range of complex control and planning tasks, RL remains hindered by its reliance on meaningful reward design, referred to as *reward shaping*. Albeit intuitively appealing, shaping often requires an intimidating amount of engineering via trial and error to yield natural-looking behaviours and makes the system prone to premature convergence to local minima (Ng et al., 1999).

Imitation learning breaks free from the preliminary reward function hand-crafting step as it does not need access to a reinforcement signal. Instead, imitation learning learns to perform a task directly from expert demonstrations. The emerging policies mimic the behaviour displayed by the expert in those demonstrations. Learning from demonstrations (LfD) has enabled significant advances in robotics (Billard et al., 2008) and autonomous driving (Pomerleau, 1989, 1990). Such models were fit from the expert demonstrations alone in a supervised fashion, without gathering new data in simulation. Albeit efficient when data is abundant, they tend to be frail as the agent strays from the expert trajectories. The ensuing compounding of errors causes a covariate shift (Ross and Bagnell, 2010; Ross et al., 2011). This approach, referred to as *behavioral cloning*, is therefore poorly adapted for imitation. Those limitations stem from the sequential nature of the problem.

The caveats of behavioral cloning have recently been successfully addressed by Ho and Ermon (Ho and Ermon, 2016) who introduced a model-free imitation learning method called *Generative Adversarial Imitation Learning* (GAIL). Leveraging Generative Adversarial Networks (GAN) (Goodfellow et al., 2014), GAIL alleviates the limitations of the supervised approach by a) learning a reward function that explains the behaviour shown in the demonstrations and b) following an RL procedure in an inner loop, consisting in performing rollouts in a simulated environment with the learned reward function as reinforcement signal. Several works have built on GAIL to overcome the weaknesses it

inherits from GANs, with a particular emphasis on avoiding the mode collapse (Goodfellow, 2017), resulting in policies that fail to display a diversity of demonstrated behaviours or skills. We do not tackle the mode collapse problem in this paper. Works that do attempt to overcome this limitation (Li et al., 2017; Hausman et al., 2017; Kuefler and Kochenderfer, 2017) fall short of addressing the sample inefficiency of GAIL and therefore still necessitate a considerable amount of interactions with the simulated environment. In this paper, we tackle this sample inefficiency limitation. Note that ‘sample efficient’ here means that we focus on limiting the number of agent-environment interactions, as opposed to reducing the number of expert demonstrations needed by the agent. Albeit important, limiting the number of needed demonstrations is not in the direct scope of this work.

Failures of previous works to address the exceeding sample complexity stems from the on-policy nature of the RL procedure they employ. Specifically, in likelihood ratio policy gradient methods, every interaction in a given rollout is used to compute the Monte Carlo estimate of the state value by summing the rewards accumulated during the current trajectory. The experienced *transitions* (atomic unit of interaction in RL) are then disregarded. Holding on to past trajectories to carry out more than a single optimization step might appear viable but often results to destructively large policy updates (Schulman et al., 2017). Gradients based on those estimates therefore suffer from high variance, which can be reduced by intensifying the sampling, hence the deterring sample efficiency.

In this work, we deal with this sample inefficiency in the number of simulator queries by leveraging a policy gradient method with function approximation (Sutton et al., 1999), referred to as *actor-critic* methods. By designing an off-policy learning procedure relying on the use of retained past experiences, we considerably shrink the amount of interactions necessary to learn good imitation policies. We build on *Deep Deterministic Policy Gradients* (Lillicrap et al., 2015), a state-of-the-art off-policy actor-critic method based on deterministic policy gradients. This also allows us to exploit further information involving the learned reward function, such its gradient. Previous methods either ignore it by treating the reward signal as a scalar in a model-free fashion or build a model of the environment to exploit it. Our method achieves the best of both worlds as it can perform a backward pass from the discriminator to the generator (policy) while remaining model-free.

2 Related Work

Imitation learning aims to learn how to perform tasks solely from expert demonstrations. Two approaches are typically adopted to tackle imitation learning problem: a) *behavioral cloning* (BC) (Pomerleau, 1989, 1990), which learns a policy via regression on the state-action pairs from the expert trajectories, and b) *apprenticeship learning* (AL) (Abbeel and Ng, 2004), which posits the existence of some unknown reward function under which the expert policy is optimal and learns a policy by i) recovering the reward that the expert is assumed to maximise (an approach called *inverse reinforcement learning* (IRL)) and ii) running an RL procedure with this recovered signal. As a supervised approach, BC is limited to the available demonstrations to learn a regression model, whose predictions worsen drastically as the agent strays from the demonstrated trajectories. It then becomes increasingly difficult for the model to recover as the errors compound (Ross and Bagnell, 2010; Ross et al., 2011; Bagnell, 2015). Only the presence of correcting behaviour in the demonstration dataset can allow BC to produce robust policies. AL alleviates this weakness by entangling learning the reward function and learning the mimicking policy, leveraging the return of the latter to adjust the parameters of the former. Models are trained on traces of interaction with the environment rather than on a fixed state pool, leading to greater generalization to states absent from the demonstrations. Albeit preventing errors from compounding, IRL comes with a high computational cost, as both modelling the reward function and solving the ensuing RL problem (per learning iteration) can be resource intensive (Syed et al., 2008; Syed and Schapire, 2008; Ho et al., 2016; Levine et al., 2011).

In an attempt to overcome the shortcomings of IRL, Ho and Ermon (Ho and Ermon, 2016) managed to bypass the need for learning the reward function assumed to have been optimised by the expert when collecting the demonstrations. The proposed approach to AL, *Generative Adversarial Imitation Learning* (GAIL), relies on an essential step consisting in learning a surrogate function measuring the similarity between the learned policy and the expert policy, using Generative Adversarial Networks (Goodfellow et al., 2014). The learned similarity metric is then employed as a reward proxy to carry out the RL step, preserved from the AL learning scheme. Recently, connections have been drawn between GANs, RL (Pfau and Vinyals, 2016) and IRL (Finn et al., 2016). In this work, we extend

GAIL to further exploit the connections between those frameworks and overcome a limitation that was left unaddressed: the burdensome sample inefficiency of the method.

Generative adversarial networks are, under their original formulation, involving a generator and a discriminator each represented by a neural network, making the associated computational graph fully differentiable. In particular, the gradient of the discriminator with respect to the output of the generator is of primary importance as it indicates in which direction the generator should change it order to have better chances to fool the discriminator at the next iteration. In GAIL, the generator’s role is carried out by a stochastic policy, causing the computational graph to no longer be differentiable end-to-end. Following a model-based approach, (Baram et al., 2017) is able to recover the gradient of the discriminator (learned reward function) with respect to actions (via reparametrization tricks) and with respect to states (via a forward model), making the computational graph fully differentiable. The deterministic policy gradient theorem (Silver et al., 2014), leveraged by our method, enables us to directly involve the gradient of the discriminator with respect to the actions to guide our mimicking agent. However, since we adopt a model-free approach, states remain stochastic nodes in the computational graph and therefore block (backward) gradient flows.

3 Background

Setting We address the problem of an agent learning to act in an environment in order to reproduce the behaviour of an expert demonstrator. No direct supervision is provided to the agent — she is never directly told what the optimal action is — nor does she receives a reinforcement signal from the environment upon interaction. Instead, the agent is provided with a pool of trajectories and must use them to guide its learning process.

Preliminaries We model this sequential interactive problem over discrete timesteps as a *Markov decision process* (MDP) \mathbb{M} , formalised as a tuple $(\mathcal{S}, \mathcal{A}, \rho_0, p, r, \gamma)$. \mathcal{S} and \mathcal{A} respectively denote the state and action spaces. The dynamics are defined by a transition distribution with conditional density $p(s_{t+1}|s_t, a_t)$, along with ρ_0 , the density of the distribution from which the initial state is sampled. Finally, $\gamma \in (0, 1]$ denotes the discount factor and $r : \mathcal{S} \times \mathcal{A} \rightarrow \mathbb{R}$ the reward function. We consider only the fully-observable case, in which the current state can be described with the current observation $o_t = s_t$, alleviating the need to involve the entire history of observations. Although our results are presented following the previous infinite-horizon MDP, the MDPs involved in our experiments are *episodic*, with $\gamma = 0$ at episode termination. In the theory, whenever we omit the discount factor, we implicitly assume the existence of an absorbing state along any trajectory generated by the agent.

We formalise the sequential decision making process of the agent by defining a parameterised policy π_θ , modelled via a neural network with parameter θ . $\pi_\theta(a_t|s_t)$ designates the conditional probability density concentrated at action a_t when the agent is in state s_t . In line with our setting, the agent interacts with \mathbb{M}^- , an MDP comprising every element of \mathbb{M} except its reward function r . Since our approach involves learning a surrogate reward function, we define \mathbb{M}^+ , denoting the MDP resulting from the augmentation of \mathbb{M}^- with the learned reward. We can therefore equivalently assume that the agent interacts with \mathbb{M}^+ . *Trajectories* are traces of interaction between an agent and an MDP. Specifically, we model trajectories as sequences of *transitions* (s_t, a_t, r_t, s_{t+1}) , atomic units of interaction. *Demonstrations* are provided to the agent through a set of expert trajectories τ_e , generated by an expert policy π_e in \mathbb{M} . Note that we adopt the RL definition of transition, as opposed to depicting a transition via a state-action pair as customarily assumed in IL. This preliminary modelling choice allows us to formally manipulate entities from both worlds that our method employs.

In fine, we introduce concepts and notations that will be instrumental in the remainder of this work. The *return* is the total discounted reward from timestep t onwards: $R_t^\gamma \triangleq \sum_{k=t}^{+\infty} \gamma^{k-t} r(s_k, a_k)$, with $\gamma \in (0, 1]$. The state-action value, or Q-value, is the expected return after picking action a_t in state s_t , and thereafter following policy π_θ : $Q^{\pi_\theta}(s_t, a_t) \triangleq \mathbb{E}_{\pi_\theta}^{>t}[R_t^\gamma]$, where $\mathbb{E}_{\pi_\theta}^{>t}[\cdot]$ denotes the expectation taken along trajectories generated by π_θ in \mathbb{M}^+ (respectively $\mathbb{E}_{\pi_e}^{>t}[\cdot]$ for π_e in \mathbb{M}) and looking onwards from state s_t and action a_t . We want our agent to find a policy π_θ that maximises the expected return from the start state, which constitutes our performance objective, $J(\pi) \triangleq \mathbb{E}_\pi[R_0^\gamma]$, i.e. $\pi_\theta = \operatorname{argmax}_\pi J(\pi)$. To ease further notations, we finally introduce the *discounted state visitation distribution* of a policy π , denoted by $\rho^\pi : \mathcal{S} \rightarrow [0, 1]$, and defined by $\rho^\pi(s) \triangleq \sum_{t=0}^{+\infty} \gamma^t \mathbb{P}_{\rho_0, \pi}[s_t = s]$, where $\mathbb{P}_{\rho_0, \pi}[s_t = s]$ is the probability of arriving at state s at time

step t when sampling the initial state from ρ_0 and thereafter following policy π . In our experiments, we omit the discount factor for state visitation, in line with common practices.

4 Algorithm

Adversarial Inverse Reinforcement Learning GAIL (Ho and Ermon, 2016) strays from previous apprenticeship learning approaches as it does not explicitly attempt to learn the reward function the demonstrator is assumed to optimise. Rather, the IRL step of GAIL learns a similarity metric between agent and expert, which then serves as a synthetic reinforcement signal to guide the policy learned in the RL step. Specifically, GAIL solves the IRL sub-problem by leveraging a new architecture inspired from GANs (Goodfellow et al., 2014). In the proposed framework, the agent mimics the behaviour of an expert by adopting a policy π_θ that matches the expert policy π_e .

Leveraging a GAN to learn a surrogate reward, GAIL introduces an extra neural network D_ϕ to play the role of *discriminator*, while the role of *generator* is carried out by the policy π_θ . D_ϕ tries to accurately assert whether a given state-action pair originates from trajectories of π_θ or π_e , while π_θ attempts to fool D_ϕ into believing her state-action pairs come from π_e . The situation can be described as a minimax problem $\min_\theta \max_\phi V(\theta, \phi)$, where the *value* of the two-player adversarial game is:

$$V(\theta, \phi) \triangleq \mathbb{E}_{\pi_\theta} [\log(1 - D_\phi(s, a))] + \mathbb{E}_{\pi_e} [\log D_\phi(s, a)] - \lambda H(\pi_\theta) \quad (1)$$

$H(\pi_\theta) \triangleq -\mathbb{E}_{\pi_\theta} [\log \pi_\theta(a|s)]$ is the causal entropy of π_θ (Bloem and Bambos, 2014), and echoes the exploration-inducing entropy regularization from the RL literature. The optimization is however hindered by the stochasticity of π_θ , causing $V(\theta, \phi)$ to be non-differentiable with respect to θ . The solution proposed in (Ho and Ermon, 2016) consists in alternating between a gradient step (ADAM, (Kingma and Ba, 2014)) on ϕ to increase $V(\theta, \phi)$ with respect to D_ϕ , and a policy optimization step (TRPO, (Schulman et al., 2015)) on θ to decrease $V(\theta, \phi)$ with respect to π_θ . In other words, while D_ϕ is trained as a binary classifier to predict if a given state-action pair is real (from π_e) or generated (from π_θ), the policy π_θ is trained by being rewarded for successfully confusing D_ϕ into believing a generated sample is coming from π_e . The reward is defined as the negative of the generator loss. As for the latter, the former can be stated in two variants, which we go over and discuss in supplementary material. In fine, adversarial IRL yields $r_\phi(s_t, a_t) = -\log(1 - D_\phi(s_t, a_t))$ as synthetic reward.

Another approach to overcome the non-differentiability of $V(\theta, \phi)$ with respect to θ is explored in (Baram et al., 2017), who plugs a forward model of the MDP \mathbb{M}^- into the model-free GAIL setting to gain full differentiability of the stochastic computational graph. Our model however only seeks differentiability of the discriminator with respect to actions in order to extract more information about how to adjust the policy parameters θ to fool D_ϕ than TRPO, which treats the learned reward as a scalar. We achieve this by leveraging *deterministic policy gradients* (DPG) (Silver et al., 2014). Specifically, we employ an off-policy deterministic actor-critic architecture built on DPG (DDPG, (Lillicrap et al., 2015)), which also allows us to achieve greater sample efficiency.

Deterministic Policy Gradients Actor-Critic (AC) methods interleave *policy evaluation* with *policy iteration*. Policy evaluation estimates the state-action value function with a function approximator called *critic* $Q_\psi \approx Q^{\pi_\theta}$, usually via either Monte-Carlo (MC) estimation or Temporal Difference (TD) learning. Policy iteration updates the policy π_θ by greedily optimising it against the estimated critic Q_ψ . Recent work showed that using off-policy TD learning for the critic, by means of experience replay, yields significant gains in sample efficiency (Silver et al., 2014). Additionally, a recent ablation study (Hessel et al., 2017) for the specific case of DQN (Mnih et al., 2013, 2015), hints that approaches such as n -step returns might be instrumental in improving the sample efficiency of off-policy actor-critic methods even further. We build on DDPG to a) bring the sample efficiency of off-policy actor-critic methods to GAIL and b) leverage gradient information hitherto disregarded.

As the name states, DDPG (Lillicrap et al., 2015) employs deterministic policies: at a given state s_t , the agent acts according to its deterministic policy μ_θ and selects the action $a_t = \mu_\theta(s_t)$. Alternatively, we can obtain a deterministic policy from any stochastic policy π_θ by systematically picking the average action for a given state: $\mu_\theta(s_t) = \mathbb{E}_a [\pi_\theta(a|s_t)]$. Deterministic policies have zero variance in their predictions for a given state, translating to no exploratory behaviour. The exploration problem is therefore treated independently from how the policy is modelled, by defining a stochastic policy π_θ from the learned deterministic policy μ_θ . In this work, we construct π_θ via the combination of two

fundamentally different techniques: a) by applying an adaptive perturbation to the learned weights θ (exploration by noise-injection in parameter space (Plappert et al., 2017) (Fortunato et al., 2017)) and b) by adding temporally-correlated noise sampled from a Ornstein-Uhlenbeck process \mathbb{OU} (Lillicrap et al., 2015), well-suited for control tasks involving inertia (e.g. simulated robotics and locomotion tasks). We denote the obtained policy by $\pi_{\theta} \triangleq \mu_{\tilde{\theta}} + \mathbb{OU}$, where $\tilde{\theta}$ results from applying a) to θ .

Our model, that we call SAM (Sample-efficient Adversarial Mimic), is a new imitation learning technique that combines deterministic policy gradients with an adversarial reward learning procedure and requires significantly fewer interactions with the environment to mimic expert behaviours. SAM is composed of three interconnected learning modules: the *reward module* (parameter ϕ), the *policy module* (parameter θ), and the *critic module* (parameter ψ) (FIGURE 1). As an off-policy method, SAM cycles through the following steps: i) the SAM agent uses π_{θ} to interact with \mathbb{M}^+ , ii) stores the experienced transitions in a replay buffer \mathcal{R} , iii) samples a mini-batch \mathcal{B} of transitions from \mathcal{R} using the off-policy distribution β , and iv) updates her parameters (θ , ψ and ϕ) by performing a training step over \mathcal{B} . A more detailed description of the training procedure is laid out in the algorithm pseudo-code (ALGORITHM 1).

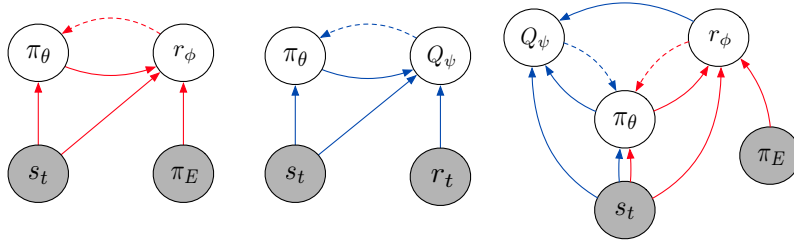


Figure 1: Inter-module relationships in different neural architectures (the scope of this figure was inspired from (Pfau and Vinyals, 2016)). Modules with distinct loss functions are depicted with empty circles, while filled circles designate environmental entities. Solid and dotted arrows respectively represent (forward) flow of information and (backward) flow of gradient. *Left*: Generative Adversarial Imitation Learning (Ho and Ermon, 2016) *Middle*: Actor-Critic architecture (Sutton et al., 1999) *Right*: SAM (this work). Note that in SAM, the critic takes in information from the reward module, while in the vanilla AC architecture, the critic receives the reward from the environment. The gradient flow from the critic to the reward module must however be sealed. Indeed, such a gradient flow would allow the policy to adjust its parameters to induces values of the reward which yield low TD residuals, hence preventing both critic and reward modules to be learned as intended.

The reward and policy modules are both involved in a GAN’s adversarial training procedure, while the policy and critic modules are trained as an actor-critic architecture. As reminded recently in (Pfau and Vinyals, 2016), GANs and actor-critic architectures can be both framed as bilevel optimization problems, each involving two competing components, which we just listed out for both architectures. Interestingly, the policy module plays a role in both problems, tying the two bilevel optimization problems together. In one problem, the policy module is trained against the reward module, while in the other, the policy module is trained against the critic module. The reward and critic modules can therefore be seen as serving analogous roles in their respective bilevel optimization problems: forging and maintaining a signal which enables the reward-seeking policy to adopt the desired behaviour. The exhibited analogy translates into both modules having analogous contributions in the gradient estimation of the performance objective, employed to update the policy parameters θ :

$$\nabla_{\theta} J(\mu_{\theta}) \approx \mathbb{E}_{s_t \sim \rho^{\beta}} \left[(1 - \zeta) \nabla_{\theta} \mu_{\theta}(s_t) \nabla_a Q_{\psi}(s_t, a)|_{a=\mu_{\theta}(s_t)} + \zeta \nabla_{\theta} \mu_{\theta}(s_t) \nabla_a r_{\phi}(s_t, a)|_{a=\mu_{\theta}(s_t)} \right] \quad (2)$$

where $\zeta \in [0, 1]$ is a hyperparameter representing the relative importance we assign to each contribution. As a reminder, $\mathbb{E}_{s_t \sim \rho^{\beta}}[\cdot]$ signifies that transitions are sampled off-policy from the replay buffer \mathcal{R} . This gradient estimation stems from the policy gradient theorem proved by (Silver et al., 2014), augmented by the previously exposed semantic analogy with a term involving another estimate of how well the agent is behaving: the learned surrogate reward r_{ϕ} . Each estimate (r_{ϕ} and Q_{ψ}) is trained via a different policy evaluation method, each presenting their specific advantages. The first is updated by adversarial training, providing an accurate estimate of the immediate similarity with

expert trajectories. The second however is trained via TD-learning, enabling longer propagation of rewards along trajectories and effectively tackling the credit assignment problem.

Given that the policy is deterministic, we can adopt an off-policy TD-learning procedure to fit the critic (Lillicrap et al., 2015), therefore learning the critic solely with samples from \mathcal{R} . The loss optimised by the critic, noted $\ell(\psi)$, involves three components: i) a 1-step Bellman residual $\ell_1(\psi)$, ii) a n -step Bellman residual $\ell_n(\psi)$, and iii) a weight decay regulariser $\mathfrak{R}(\psi)$ (Večerík et al., 2017) employs the same losses in the context of RLfD, but also uses a weight decay regulariser for the policy):

$$\ell(\psi) \triangleq \ell_1(\psi) + \ell_n(\psi) + \nu \mathfrak{R}(\psi) \quad (3)$$

where ν is a hyperparameter that determines how much decay is used. The losses i) and ii) are defined respectively based on the 1-step and n -step lookahead versions of the Bellman equation,

$$\tilde{Q}_\psi^1(s_t, a_t) \triangleq r_\phi(s_t, a_t) + \gamma Q_\psi(s_{t+1}, \mu_\theta(s_{t+1})) \quad (4)$$

$$\tilde{Q}_\psi^n(s_t, a_t) \triangleq \sum_{k=0}^{n-1} \gamma^k r_\phi(s_{t+k}, a_{t+k}) + \gamma^n Q_\psi(s_{t+n}, \mu_\theta(s_{t+n})) \quad (5)$$

yielding the critic losses:

$$\ell_1(\psi) \triangleq \mathbb{E}_{s_t \sim \rho^\beta, a_t \sim \beta}[(\tilde{Q}_\psi^1 - Q_\psi)^2(s_t, a_t)] \quad \ell_n(\psi) \triangleq \mathbb{E}_{s_t \sim \rho^\beta, a_t \sim \beta}[(\tilde{Q}_\psi^n - Q_\psi)^2(s_t, a_t)] \quad (6)$$

Both Q_ψ and \tilde{Q}_ψ ((4), (5)) depend on ψ , which might cause severe instability. In order to prevent the critic from diverging, we use separate *target* networks for both policy and critic (θ' , ψ') to calculate \tilde{Q}_ψ , which slowly track the learned parameters (θ , ψ). We also found that using a n -step TD backup was necessary for our method to learn well-behaved policies.

Algorithm 1: SAM: Sample-efficient Adversarial Mimic

```

1 Initialise replay buffer  $\mathcal{R}$ 
2 Initialise network parameters for each module ( $\phi$ ,  $\theta$ ,  $\psi$ )
3 Initialise target network parameters ( $\theta'$ ,  $\psi'$ ) as respective copies of ( $\theta$ ,  $\psi$ )
4 for  $i \in 1, \dots, i_{\max}$  do
5   for  $c \in 1, \dots, c_{\max}$  do
6     // Collect and store samples from environment
7     Interact with environment following  $\pi_\theta$ 
8     Store experienced transition in replay buffer  $\mathcal{R}$ 
9   end
10  for  $t \in 1, \dots, t_{\max}$  do
11    # Update SAM
12    for  $d \in 1, \dots, d_{\max}$  do
13      // Update (d)iscriminator (synthetic reward)
14      Sample minibatch  $\mathcal{B}^d$  of previously experienced transitions from  $\mathcal{R}$ 
15      Sample minibatch  $\mathcal{B}_e^d$  of transitions from the expert dataset  $\tau_e$ , such that  $|\mathcal{B}^d| = |\mathcal{B}_e^d|$ 
16      Update synthetic reward parameter  $\phi$  with the equal mixture  $\mathcal{B}^d \cup \mathcal{B}_e^d$  by following the
17      gradient:  $\mathbb{E}_{(s,a) \sim \mathcal{B}^d}[\nabla_\phi \log(1 - D_\phi(s, a))] + \mathbb{E}_{(s,a) \sim \mathcal{B}_e^d}[\nabla_\phi \log D_\phi(s, a)]$ 
18    end
19    for  $g \in 1, \dots, g_{\max}$  do
20      // Update (g)enerator (actor-critic)
21      Sample minibatch  $\mathcal{B}^g$  of previously experienced transitions from  $\mathcal{R}$ 
22      Update policy parameter  $\theta$  by following the gradient:  $\mathbb{E}_{(s,a) \sim \mathcal{B}^g}[\nabla_\theta J(\mu_\theta)(s, a)]$ 
23      Update critic parameters  $\psi$  by minimizing critic loss:  $\mathbb{E}_{(s,a) \sim \mathcal{B}^g}[\ell(\psi)(s, a)]$ 
24      Update target network parameters ( $\theta'$ ,  $\psi'$ ) to slowly track ( $\theta$ ,  $\psi$ ), respectively
25    end
26  end
27 end

```

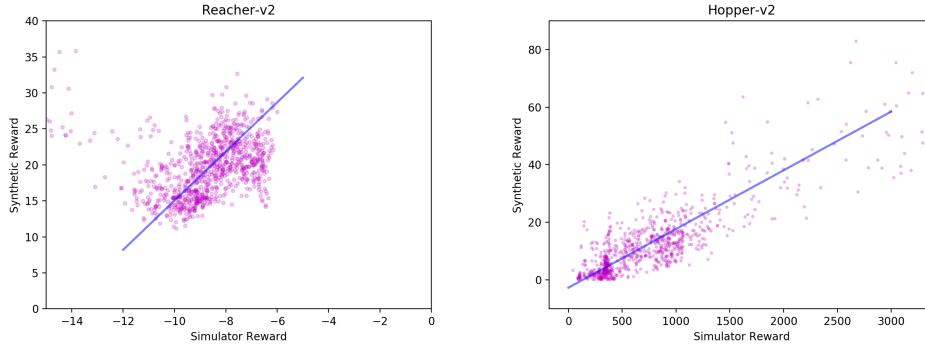


Figure 2: Evaluation of the reward module. The regression line supports our claim: the surrogate reward, learned solely from expert demonstrations, is a good proxy of the true simulator reward.

5 Results

Our agents were trained in physics-based control environments, built with the MUJoCo physics engine (Todorov et al., 2012), and wrapped via the OpenAI Gym (Brockman et al., 2016) API. Tasks simulated in the environments range from legacy balance-oriented tasks to locomotion tasks of various complexities. Time and resource constraints led us to consider the 4 first environments when ordered by increasing complexity: InvertedPendulum (Cartpole), InvertedDoublePendulum (Acrobot), Reacher and Hopper. For each environment, an expert was designed by training an agent for 10M timesteps using the TRPO (Schulman et al., 2015) implementation from (Dhariwal et al., 2017). The episode horizon (maximum episode length) was left to its default value per environment. We created a dataset of expert trajectories per environment. Trajectories are not limited in length but often coincide with the episode horizon, due to the good performance of the experts. Moreover, they are extracted without randomisation, which ensures that two compared models are trained on exactly the same subset of extracted trajectories.

Since we claim to improve the sample efficiency of GAIL (Ho and Ermon, 2016) and, to the best of our knowledge, do not share this claim with other works, we will compare SAM directly to GAIL as baseline. Implementation details are provided in supplementary material.

Our results are presented in FIGURE 3, which traces the evolution of the environmental reward collected by SAM and GAIL agents as they sequentially interact with the environment. For the three first environments (due to limited time and resources), we evaluated the performance of the agents when provided with various quantities of demonstrations. SAM agents consistently reach expert performance with less interactions than GAIL agent, which does not always achieve the demonstrator’s performance (e.g. in the Reacher environment). The sample-efficiency we gain over GAIL is considerable: SAM needs more than one order of magnitude less interactions with the environment to attain asymptotic expert performance. Note that the horizontal axis is scaled logarithmically. While GAIL requires full traces of agent–environment interaction per iteration as it relies on Monte-Carlo estimates, SAM only requires a couple of transitions per iteration since it performs policy evaluation via Temporal Difference learning. Instead of sampling transitions from the environment, performing an update and discarding the transitions, SAM keeps experiential data in memory and can therefore leverage decorrelated transitions collected in previous iterations to perform an off-policy update. Our method therefore requires considerably fewer new samples (interactions) per iteration, as it can re-exploit the transitions previously experienced.

For the two first environments, GAIL and SAM have comparable wall-clock time. As the tasks become more complex however, SAM’s wall clock time becomes greater, which is explained by the number of sub-iterations our method performs on the replay buffer per iteration, not involving any new samples. On the Reacher task, GAIL took a tremendous amount of iterations to assimilate the demonstrated skill and reproduce a similar behaviour, without even fully reaching the expert’s performance. Training duration were therefore in favour of SAM. For the Hopper environment however, while a GAIL agent takes on average 1.5 hours to adopt an expert-like behaviour, a SAM

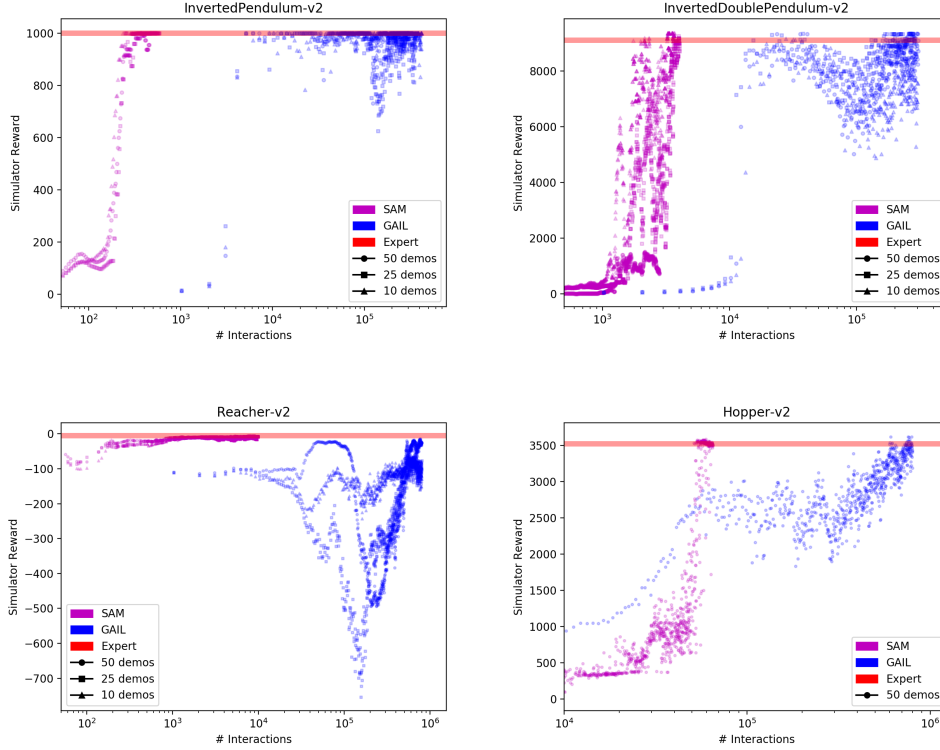


Figure 3: Performance comparison between SAM and GAIL. The markers represent the number of expert trajectories the agent had access to. The figure shows that our method has a considerably better sample-efficiency than GAIL in the explored set of environments. Note that the horizontal axis has a logarithmic scale. We remind the reader that ‘demonstration’ here means ‘expert trajectory’. The number of interactions have been averaged over the pool of parallel workers used to run the experiment (32). High-resolution versions of these plots are provided in supplementary material.

agent takes approximatively 30 hours. While these results shed light on a clear trade-off between wall-clock time and number of interactions, we claim that in real-world scenarios (e.g. robotic manipulation, autonomous cars), reducing the required interaction with the world is significantly more desirable, for obvious safety and cost reasons. We report the hyperparameters used in our experiments in supplementary material.

The gradient in EQUATION (2) involves $\zeta \in [0, 1]$. In this work, we only present results for $\zeta = 0$, as the preliminary experiments we conducted with $\zeta \in (0, 1]$ have not lead to expert-like policies. Time and resource constraints however did not allow for a full exploration of this tradeoff. We therefore leave further investigation for future work.

6 Conclusion

In this work, we introduced a method, called *Sample-efficient Adversarial Mimic* (SAM), that meaningfully overcomes one considerable drawback of the *Generative Adversarial Imitation Learning* (Ho and Ermon, 2016) algorithm: the number of agent–environment interactions it requires to learn expert-like policies. We demonstrate that our method shrinks the number of interactions by an order of magnitude, and sometimes more. Leveraging an off-policy procedure was key to that success.

References

- Abbeel, P. and Ng, A. Y. (2004). Apprenticeship Learning via Inverse Reinforcement Learning. In *Proceedings of the 21st International Conference on Machine Learning (ICML)*.
- Ba, J. L., Kiros, J. R., and Hinton, G. E. (2016). Layer Normalization.
- Bagnell, J. A. (2015). An invitation to imitation. Technical report, Carnegie Mellon, Robotics Institute, Pittsburgh.
- Baram, N., Anschel, O., Caspi, I., and Mannor, S. (2017). End-to-End Differentiable Adversarial Imitation Learning. In *Proceedings of the 34th International Conference on Machine Learning (ICML)*, pages 390–399.
- Billard, A., Calinon, S., Dillmann, R., and Schaal, S. (2008). Robot Programming by Demonstration. In Bruno, S. and Oussama, K., editors, *Springer Handbook of Robotics*, pages 1371–1394. Springer Berlin Heidelberg.
- Bloem, M. and Bambos, N. (2014). Infinite time horizon maximum causal entropy inverse reinforcement learning. In *53rd IEEE Conference on Decision and Control (CDC)*, pages 4911–4916.
- Brockman, G., Cheung, V., Pettersson, L., Schneider, J., Schulman, J., Tang, J., and Zaremba, W. (2016). OpenAI Gym.
- Dhariwal, P., Hesse, C., Plappert, M., Radford, A., Schulman, J., Sidor, S., and Wu, Y. (2017). Openai baselines.
- Fedus, W., Rosca, M., Lakshminarayanan, B., Dai, A. M., Mohamed, S., and Goodfellow, I. (2017). Many Paths to Equilibrium: GANs Do Not Need to Decrease a Divergence At Every Step.
- Finn, C., Christiano, P., Abbeel, P., and Levine, S. (2016). A Connection between Generative Adversarial Networks, Inverse Reinforcement Learning, and Energy-Based Models.
- Fortunato, M., Azar, M. G., Piot, B., Menick, J., Osband, I., Graves, A., Mnih, V., Munos, R., Hassabis, D., Pietquin, O., Blundell, C., and Legg, S. (2017). Noisy Networks for Exploration.
- Goodfellow, I. (2017). NIPS 2016 Tutorial: Generative Adversarial Networks.
- Goodfellow, I., Pouget-Abadie, J., Mirza, M., Xu, B., Warde-Farley, D., Ozair, S., Courville, A., and Bengio, Y. (2014). Generative Adversarial Nets. In *Advances in Neural Information Processing Systems 27 (NIPS)*, pages 2672–2680.
- Hausman, K., Chebotar, Y., Schaal, S., Sukhatme, G., and Lim, J. (2017). Multi-Modal Imitation Learning from Unstructured Demonstrations using Generative Adversarial Nets.
- Hessel, M., Modayil, J., van Hasselt, H., Schaul, T., Ostrovski, G., Dabney, W., Horgan, D., Piot, B., Azar, M., and Silver, D. (2017). Rainbow: Combining Improvements in Deep Reinforcement Learning.
- Ho, J. and Ermon, S. (2016). Generative Adversarial Imitation Learning.
- Ho, J., Gupta, J. K., and Ermon, S. (2016). Model-Free Imitation Learning with Policy Optimization.
- Kingma, D. P. and Ba, J. (2014). Adam: A Method for Stochastic Optimization.
- Kuefler, A. and Kochenderfer, M. J. (2017). Burn-In Demonstrations for Multi-Modal Imitation Learning.
- Levine, S., Popovic, Z., and Koltun, V. (2011). Nonlinear Inverse Reinforcement Learning with Gaussian Processes. In *Advances in Neural Information Processing Systems 24 (NIPS)*, pages 19–27.
- Li, Y., Song, J., and Ermon, S. (2017). Inferring The Latent Structure of Human Decision-Making from Raw Visual Inputs.

- Lillicrap, T. P., Hunt, J. J., Pritzel, A., Heess, N., Erez, T., Tassa, Y., Silver, D., and Wierstra, D. (2015). Continuous control with deep reinforcement learning.
- Mnih, V., Kavukcuoglu, K., Silver, D., Graves, A., Antonoglou, I., Wierstra, D., and Riedmiller, M. (2013). Playing Atari with Deep Reinforcement Learning.
- Mnih, V., Kavukcuoglu, K., Silver, D., Rusu, A. A., Veness, J., Bellemare, M. G., Graves, A., Riedmiller, M., Fidjeland, A. K., Ostrovski, G., Petersen, S., Beattie, C., Sadik, A., Antonoglou, I., King, H., Kumaran, D., Wierstra, D., Legg, S., and Hassabis, D. (2015). Human-level control through deep reinforcement learning. *Nature*, 518(7540):529–533.
- Ng, A. Y., Harada, D., and Russell, S. (1999). Policy invariance under reward transformations: Theory and application to reward shaping. In *Proceedings of the 16th International Conference on Machine Learning (ICML)*, pages 278–287.
- Pfau, D. and Vinyals, O. (2016). Connecting Generative Adversarial Networks and Actor-Critic Methods.
- Plappert, M., Houthoofd, R., Dhariwal, P., Sidor, S., Chen, R. Y., Chen, X., Asfour, T., Abbeel, P., and Andrychowicz, M. (2017). Parameter Space Noise for Exploration.
- Pomerleau, D. (1989). ALVINN: An Autonomous Land Vehicle in a Neural Network. In *Advances in Neural Information Processing Systems 1*, pages 305–313.
- Pomerleau, D. (1990). Rapidly Adapting Artificial Neural Networks for Autonomous Navigation. In *Advances in Neural Information Processing Systems 3 (NIPS)*, pages 429–435.
- Ross, S. and Bagnell, J. A. (2010). Efficient Reductions for Imitation Learning. In *International Conference on Artificial Intelligence and Statistics (AISTATS)*, pages 661–668. jmlr.org.
- Ross, S., Gordon, G. J., and Bagnell, J. A. (2011). A Reduction of Imitation Learning and Structured Prediction to No-Regret Online Learning. In *International Conference on Artificial Intelligence and Statistics (AISTATS)*, pages 627–635. jmlr.org.
- Schulman, J., Levine, S., Moritz, P., Jordan, M. I., and Abbeel, P. (2015). Trust Region Policy Optimization. In *Proceedings of the 32nd International Conference on Machine Learning (ICML)*.
- Schulman, J., Wolski, F., Dhariwal, P., Radford, A., and Oleg, K. (2017). Proximal Policy Optimization Algorithms.
- Silver, D., Lever, G., Heess, N., Degris, T., Wierstra, D., and Riedmiller, M. (2014). Deterministic Policy Gradient Algorithms. In *Proceedings of the 31st International Conference on Machine Learning (ICML)*, pages 387–395.
- Sutton, R. S. and Barto, A. G. (2017). Reinforcement Learning: An introduction (Latest draft, 2nd Edition).
- Sutton, R. S., McAllester, D. A., Singh, S. P., and Mansour, Y. (1999). Policy Gradient Methods for Reinforcement Learning with Function Approximation. In *Advances in Neural Information Processing Systems 12 (NIPS)*, pages 1057–1063.
- Syed, U., Bowling, M., and Schapire, R. E. (2008). Apprenticeship Learning Using Linear Programming. In *Proceedings of the 25th International Conference on Machine Learning (ICML)*, pages 1032–1039.
- Syed, U. and Schapire, R. E. (2008). A Game-Theoretic Approach to Apprenticeship Learning. In *Advances in Neural Information Processing Systems 20 (NIPS)*, pages 1449–1456.
- Todorov, E., Erez, T., and Tassa, Y. (2012). MuJoCo: A physics engine for model-based control. In *IEEE/RSJ International Conference on Intelligent Robots and Systems (IROS)*, pages 5026–5033.
- van Hasselt, H., Guez, A., Hessel, M., Mnih, V., and Silver, D. (2016). Learning values across many orders of magnitude.
- Večerík, M., Hester, T., Scholz, J., Wang, F., Pietquin, O., Piot, B., Heess, N., Rothörl, T., Lampe, T., and Riedmiller, M. (2017). Leveraging Demonstrations for Deep Reinforcement Learning on Robotics Problems with Sparse Rewards.

A Studied environments

The environments we dealt were provided through the OpenAI Gym (Brockman et al., 2016) API, building on the MUJoCo physics engine (Todorov et al., 2012), to model physical interactive scenarios between an agent and the environment she is thrown into. The control tasks modelled by the environments involve locomotion tasks as well as tasks in which the agent must reach and remain in a state of dynamic balance.

Environment	State DoFs	Action DoFs
InvertedPendulum-v2	4	1
InvertedDoublePendulum-v2	11	1
Reacher-v2	11	2
Hopper-v2	11	3

Figure 4: Degrees of freedom (DoF) of the 4 considered MUJoCo simulated environments. DoFs of both continuous action and state spaces are presented, for the studied physical control tasks. Actions spaces are bounded along every dimension, while the state spaces are unbounded.

B Reward function variants

The reward is defined as the negative of the generator loss. As for the latter, the former can be stated in two variants, the saturating version and the non-saturating version, respectively

$$r_{\phi}^{\wedge}(s_t, a_t) = -\log(1 - D_{\phi}(s_t, a_t)) \quad r_{\phi}^{\sim}(s_t, a_t) = \log D_{\phi}(s_t, a_t) \quad (7)$$

The non-saturating alternative is recommended in the original GAN paper as well as in (Fedus et al., 2017) more recently, as the generator loss suffers from vanishing gradients only in areas where the generated samples are already close to the real data. GAIL relies on policy optimization to update the generator, which makes this vanishing gradient argument vacuous. Besides, in the context of simulated locomotion environments, the saturated version proved to prevail in our experiments, as our agents were unable to overcome the extremely low rewards incurred early in training when using the non-saturating rewards. With the saturated version, signals obtained in early failure cases were close to zero, which was more numerically forgiving for our agents to kick off.

C Experimental setup

Our algorithm and baseline implement the MPI interface: each experiment has been launch concurrently with 32 parallel workers (32 different seeds), each having its own interaction with the environment, its own replay buffer, its own optimisers and its own network updates. However, every iteration and for a given network (e.g. the critic), the gradients of the 32 ADAM (Kingma and Ba, 2014) optimisers are pulled together, averaged, and a unique average gradient is distributed to the worker for immediate usage. We rely on the MPI-optimised ADAM optimiser available at the OpenAI Baselines (Dhariwal et al., 2017) repository, released to enhance and encourage reproducibility. Our experiments have all been conducted relying solely on a single 16-core CPU workstation (AMD Ryzen™ Threadripper 1950X CPU). We are currently working on gaining access to GPU infrastructures to fully take advantage of the off-policy nature of SAM, and will then repurpose the CPU threads to focus exclusively on simulator query.

The implementation of GAIL we used takes inspiration from the original implementation as well as from the GAIL implementation recently integrated to (Dhariwal et al., 2017), itself stemming from the original implementation. Hyperparameters of the core algorithm are preserved in our implementation of the baseline (table provided in supplementary material). Additionally, both SAM and GAIL implementations use exactly the same discriminator implementation, highlighting that SAM’s better sample efficiency is due to its architecture and orchestration of modules, rather than caused by a better implementation of the reward module, that both models share (e.g. by leveraging a GAN improvement).

Hyperparameter	Value
# workers	32
num demos	$\in \{10, 25, 50\}$
policy # layers	2
policy layer widths	(100, 100)
policy hidden activations	tanh
discriminator # layers	2
discriminator layer widths	(100, 100)
discriminator hidden activations	leaky ReLU
discount factor γ	0.995
generator training steps	3
discriminator training steps	1
non-saturating reward?	false
entropy regularization coefficient λ	0
# timesteps (interactions) per iteration	1000
minibatch size	128
normalize observations?	true
# timesteps upper bound	25M (total across workers)
BC pre-training	false

Figure 5: Hyperparameters used to train GAIL agents.

D Hyperparameters settings

In our training procedure, we adopted an alternating scheme consisting in performing 3 training iterations of the actor-critic architecture for one training iteration of the synthetic reward, in line with common practises in the GAN literature (the actor-critic acts as generator, while the synthetic reward plays the role of discriminator). This training pattern applies for both the GAIL baseline and our algorithm SAM.

As supported by the ending discussion of the GAIL paper, performing a behavioral cloning (Pomerleau, 1989, 1990) pre-training step to warm-start GAIL can potentially yield expert-like policies in fewer number of ensuing GAIL training iterations. It is especially appealing in so far as the behavioral cloning agent does not interact with the environment at all while training. We therefore intended to precede the training of our experiments (for GAIL and SAM) with a behavioral cloning pre-training phase. However, although the previous training pipeline enables a reduction of training iterations for GAIL, we did not witness a consistent benefit for SAM in our preliminary experiments. Our proposed explanation of this phenomenon is that by pre-training both policy and critic individually as regression problems over the expert demonstrations dataset, we hinder the entanglement of the policy and critic training procedures exploited in SAM. We believe that by adopting a more elaborate pre-training procedure, we will be able to overcome this issue, and therefore leave further exploration for future work.

Hyperparameter	Value
# workers	32
num demos	$\in \{10, 25, 50\}$
policy # layers	2
policy layer widths	(100, 100)
policy hidden activations	leaky ReLU
policy layer normalisation (Ba et al., 2016)	true
policy output activation	tanh
critic # layers	2
critic layer widths	(100, 100)
critic hidden activations	leaky ReLU
critic layer normalisation (Ba et al., 2016)	true
discriminator # layers	2
discriminator layer widths	(100, 100)
discriminator hidden activations	leaky ReLU
discount factor γ	0.995
policy gradient interpolation factor ζ	0
generator training steps	3
discriminator training steps	1
non-saturating reward?	false
entropy regularization coefficient λ	0
# timesteps (interactions) per iteration	4
minibatch size	32
# training steps per iteration	10
replay buffer size	100K
normalise observations?	true
normalise returns?	true
POP-ART (van Hasselt et al., 2016)?	true
reward scaling factor	1000
critic weight decay regularization coefficient ν	0.001
critic 1-step TD loss coefficient	1
critic n -step TD loss coefficient	1
TD lookahead length n	100
adaptive parameter noise for π_θ	0.2
Ornstein-Uhlenbeck additive noise for π_θ	0.2
# timesteps upper bound	25M (total across workers)
BC pre-training	false

Figure 6: Hyperparameters used to train SAM agents.

E Enhanced plots

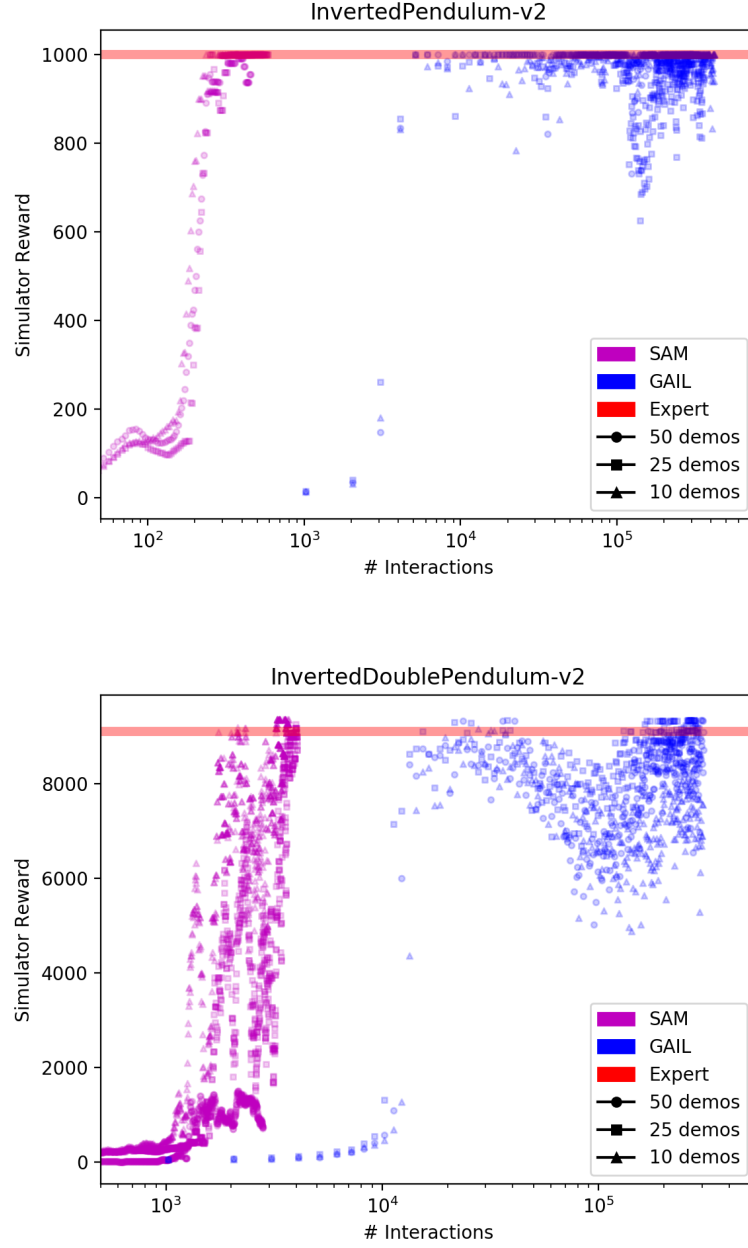


Figure 7: Performance comparison between SAM and GAIL. The markers represent the number of expert trajectories the agent had access to. The figure shows that our method has a considerably better sample-efficiency than GAIL in the explored set of environments. Note that the horizontal axis has a logarithmic scale. We remind the reader that ‘demonstration’ here means ‘expert trajectory’. The number of interactions have been averaged over the pool of parallel workers used to run the experiment (32).

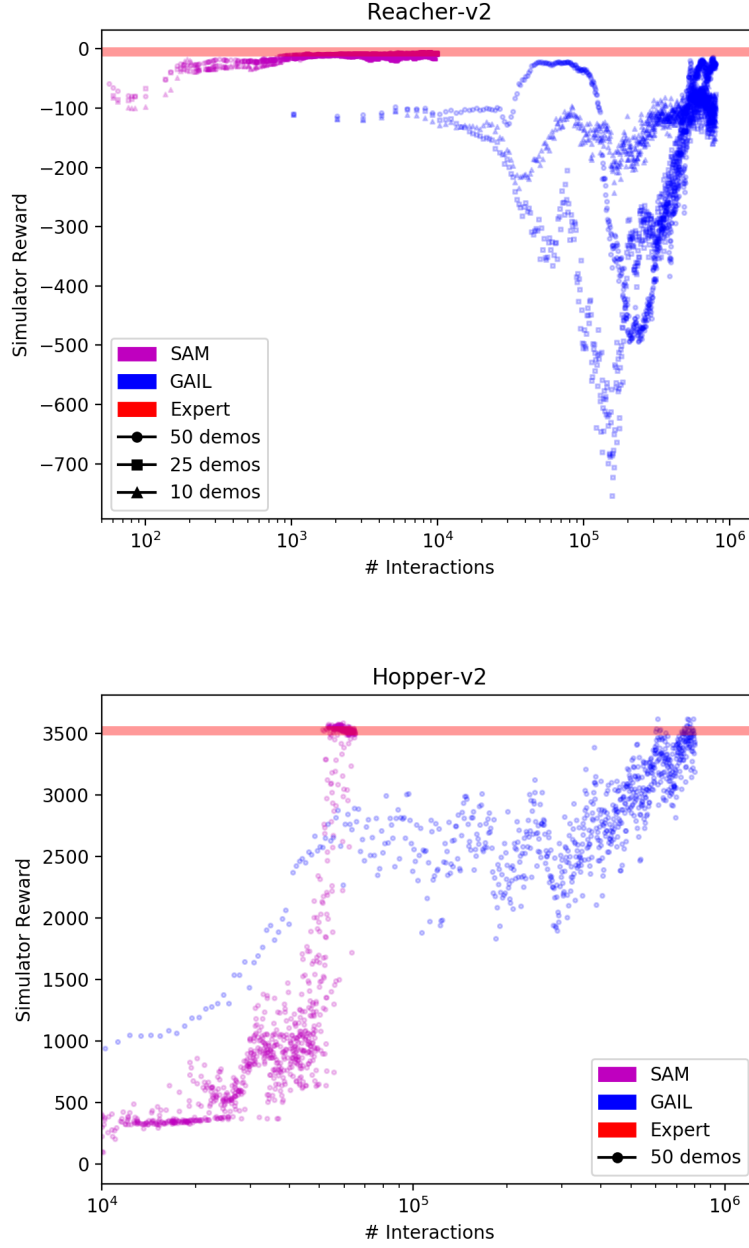


Figure 8: Performance comparison between SAM and GAIL. The markers represent the number of expert trajectories the agent had access to. The figure shows that our method has a considerably better sample-efficiency than GAIL in the explored set of environments. Note that the horizontal axis has a logarithmic scale. We remind the reader that ‘demonstration’ here means ‘expert trajectory’. The number of interactions have been averaged over the pool of parallel workers used to run the experiment (32).